PMD tolerant nonlinear compensation using in-line phase conjugation

M. E. McCarthy,[*] **M. A. Z. Al Kahteeb, F. M. Ferreira, and A. D. Ellis**

Aston Institute of Photonic Technology, Aston University, Aston Triangle, Birmingham, UK

[*]*m.mccarthy@aston.ac.uk*

Abstract: In this paper, we numerically investigate the impact of polarisation mode dispersion on the efficiency of compensation of nonlinear transmission penalties for systems employing one of more inline phase conjugation devices. We will show that reducing the spacing between phase conjugations allows for significantly improved performance in the presence polarisation mode dispersion or a significant relaxation in the acceptable level of polarization mode dispersion. We show that these results are consistent with previously presented full statistical analysis of nonlinear transmission appropriately adjusted for the reduced section length undergoing compensation.

References and links

1. I. D. Phillips, M. Tan, M. F. C. Stephens, M. E. McCarthy, E. Giacoumidis, S. Sygletos, P. Rosa, S. Fabbri, S. T. Le, T. Kanesan, S. K. Turitsyn, N. J. Doran, P. Harper, and A. D. Ellis, "Exceeding the nonlinear-Shannon Limit using Raman laser based amplification and optical phase conjugation," in *Optical Fiber Communication Conference* (2014), paper M3C.1.
2. H. Hu, R. M. Jopson, A. H. Gnauck, M. Dinu, S. Chandrasekhar, X. Liu, C. Xie, M. Montoliu, S. Randel, and C. J. McKinstrie, "Fibre nonlinearity compensation of an 8-channel WDM PDM-QPSK signal using multiple phase conjugators," in *Optical Fiber Communication Conference* (2014), paper M3C.2.
3. K. Solis-Trapala, M. D. Pelusi, H. Nguyen Tan, T. Inoue, and S. Namiki, "Transmission optimized impairment mitigation by 12 stage phase conjugation of WDM 24x48 Gb/s DP-QPSK signals," in *Optical Fiber Communication Conference* (2015), paper Th3C.2.
4. K. Solis-Trapala, M. Pelusi, H.N. Tan, T. Inoue, S. Suda, and S. Namiki, "Doubled transmission reach for DP-64QAM signal over field-deployed legacy fiber systems enabled by MSSI," in *European Conference on Optical Communication* (2015), paper Mo.3.6.2.
5. S. Yoshima, Y. Sun, K. Bottril, F. Parmigiani, P. Petropoulos, and D. J. Richardson, "Nonlinearity mitigation through optical phase conjugation in a deployed fibre link with full bandwidth utilization," in *European Conference on Optical Communication* (2015), paper We2.6.3.
6. I. Sackey, F Da Ros, J. K. Fischer, T. Richter, M. Jazayerifar, C. Peucheret, K. Petermann, and C. Schubert, "Kerr nonlinearity mitigation: Mid-link spectral inversion versus digital backpropagation in 528-GBd PDM 16-QAM signal transmission," J. Lightwave Technol. **33**, 1821–1827 (2015).
7. M. Morshed, L. B. Du, B. Foo, M. D. Pelusi, B. Corcoran, and A. J. Lowery, "Experimental demonstration of dual polarization CO-OFDM using mid-span spectral inversion for nonlinearity compensation," Opt. Express **22**, 10455 (2014).
8. A. D. Ellis, M. Tan, M. A. Iqbal, M. A. Z. Al Khateeb, V. Gordienko, G. Saavedra. M., S.Fabbri, M. F. C. Stephens, M. E. McCarthy, A. Perentos, I. D. Phillips, D. Lavery, G. Liga, R.Maher, P. Harper, N. J. Doran, S. K. Turitsyn, S. Sygletos, and P. Bayvel, "4 Tbit/s transmission reach enhancement using ten 400 Gbit/s super-channels and polarization insensitive dual band optical phase conjugation," invited submission to J. Lightwave Technol. (to be published).
9. E. M. Ip and J. M. Kahn, "Compensation of dispersion and nonlinear impairments using digital backpropagation," J. Lightwave Technol. **26**(20), 3416–3425 (2008).
10. L. F. Mollenauer and J. P. Gordon, "Birefringence mediated timing jitter in soliton transmission," Opt. Lett. **19**(6), 375 (1994).

11. R. A. Saunders , D. Garthe , B. L. Patel , W. S. Lee, and R. E. Epworth, "Observation of parametric noise amplification owing to modulation instability in anomalous dispersion regime," Electron. Lett. **31**(13), 1088–1090 (1995).
12. D. Rafique and A. D. Ellis, "Impact of signal-ASE four-wave mixing on the effectiveness of digital back-propagation in 112 Gb/s PM-QPSK systems," Opt. Express **19**, 3449 (2011).
13. G. Gao, X. Chen, and W. Shieh, "Influence of PMD on fiber nonlinearity compensation using digital back propagation," Opt. Express **20**, 14406 (2012).
14. G. Liga, T. Xu, A. Alvarado,R. I. Killey and P. Bayvel "On the performance of multichannel digital backpropagation in high-capacity long-haul optical transmission," Opt. Express **22**, 30053 (2014).
15. A. D. Ellis, S. T. Le, D. Lavery and S.K. Turitsyn, "The impact of phase conjugation on the nonlinear-Shannon Limit," in *Proceedings of Summer Topicals Meeting Series (SUM)* (2015), paper TuF3.2.
16. K. Goroshko, O. Ozolins, H. Louchet, A. Richter, "PMD-induced penalty on digital back propagation and its mitigation," private communication.
17. X.Chen, W.Shieh, "Closed form expressions for nonlinear transmission performance of densely spaced coherent optical OFDM systems," Opt. Express **16**, 19039 (2010).
18. P.Poggiolini, "Modeling of non-linear propagation in uncompensated coherent systems," in *Optical Fiber Communication Conference* (2013), paper OTh3G1.l.
19. A.D.Ellis, J. , D. Cotter, "Approaching the non-linear Shannon limit," J. Lightwave Technol. **28**, 423 (2010).
20. A Mecozzi, RJ Essiambre, "Nonlinear Shannon limit in pseudolinear coherent systems," J. Lightwave Technol. **30**, 2011 (2012).
21. P. Poggiolini, A. Carena, Y. Jiang, G. Bosco, V. Curri, F. Forghieri, Impact of low-OSNR operation on the performance of advanced coherent optical transmission systems," in *European Conference on Optical Communication* (2014), paper Mo.4.3.2.
22. Tang, Jau., "A comparison study of the Shannon channel capacity of various nonlinear optical fibers," J. Lightwave Technol. **24**, 5, 2070 (2006).
23. A. D. Ellis, M. E. McCarthy, M. A. Z. Al-Khateeb, and S. Sygletos, "Capacity limits of systems employing multiple optical phase conjugators," Opt. Express **23**, 20381 (2015).
24. T. Tanimura, M. Nlle, J. K. Fischer, and C. Schubert, "Analytical results on back propagation nonlinear compensator with coherent detection," Opt. Express **20**, 28779 (2012).
25. J. P. Gordon, H. Kogelnik, "PMD fundamentals: Polarization mode dispersion in optical fibers," Proc. Natl. Acad. Sci. U. S. A **97** (9), 4541–4550 (2000).
26. G. Biondini, W. L. Kath, and C. R. Menyuk, "Importance sampling for polarization-mode dispersion," IEEE Photonics Technol. Lett. **14** (2), 310–312 (2002).
27. A. Carena,G. Bosco, V. Curri, P. Poggiolini, M. T. Taiba, and F. Forghieri, "Statistical characterization of PM-QPSK signals after propagation in uncompensated fiber links," in *European Conference on Optical Communication* (2010), paper P4.07.

1. Introduction

As results approach the nonlinear Shannon limit, compensation of nonlinear transmission penalties in high capacity WDM systems is required to enable further capacity growth [1–9]. This is especially true for systems with higher order constellations which require a higher minimum signal to noise ratio (SNR) for a fixed FEC overhead and have lower tolerance to uncompensated distortions. These generally use a combination of digital signal processing (DSP) and Raman amplification to improve the transmission reach. Raman amplification reduces the accumulated noise compared to traditional Eribium doped fibre amplification schemes. Deterministic intra-channel impairments such as chromatic dispersion and self-phase modulation can be compensated completely using modern DSP. However, the compensation of nonlinear distortions which result from interactions with stochastic effects, such as polarisation mode dispersion (PMD) [10] and noise [11], still presents significant challenges. For long haul, dispersion unmanaged, high spectral efficiency systems the stochastic nature of PMD prevents the limit imposed by parametric noise amplification [12] being reached [13].

PMD is a stochastic effect resulting from fibre imperfections, such as geometry and stress asymmetries, causing the two polarization modes to travel with different group velocities in a single-mode fibre i.e. localised changes in fibre birefringence. These changes can be introduced either at fibre manufacturing or during cabling. Much research effort has been expended in developing techniques to minimise PMD but it is impossible to predict its local value. Under

the influence of PMD, polarisation states of different channels walk off with distance and, since nonlinear effects such as four wave mixing are strongly polarisation dependent, it becomes increasingly difficult to predict the exact nonlinear interaction.This is disruptive for electronic digital back propagation (DBP) in systems where the backpropagated bandwidth is wider than the PMD correlation bandwidth as the non-linear impairments between widely spaced wavelengths can not be definitively known at all points in the transmission link. This leads to divergence or asymmetry between the forward and back propagation and reduces the ability of DBP to compensate for nonlinearity. Once this point is reached, extending the DBP bandwidth will not lead to further improvement in performance. [14]. Preliminary studies [13–15] have confirmed that DBP performance is severely limited and have presented exact [13] and heuristic [15] calculations of the effective bandwidth of the DBP. This typically limits the performance improvement to less than 2.5 *dB* for 0.1 *ps km*$^{-1/2}$. Span by span principle state tracking has been proposed to improve the efficiency of the DBP [16], although the precise performance gain and implementation complexity have yet to be established.

Inline forms of nonlinearity compensation, such as optical phase conjugation [1–8], provide compensation of both intra and inter channel nonlinear effects. Nonlinearity compensation performance using inline phase conjugation (iPCs) depends on the symmetry between the spans preceding and following the phase conjugation element. An ideal iPC placed at the mid-point of a symmetric transmission link offers improved ideal performance over transmitter or receiver based nonlinearity compensation. It disrupts the quadratic growth of parametrically amplified noise, and halves the segment over which the signal polarisations are decorrelated, and so increasing the accuracy of the nonlinearity compensation. Experimental demonstrations have attempted to optimise both power and dispersion symmetry which have allowed for up to 70% of the signal dependent non-linearity to be compensated [1], and inline phase conjugation performed every 12 km has enabled an 8 dB increase in nonlinear threshold [3]. However, long haul experiments remain limited by the impact of PMD.

In this paper, we will show that shortening the segment to be compensated by adding additional iPCs results increases the performance even in the presence of moderately high levels of PMD. For the specific WDM system studied, we demonstrate that an approximately two fold increase in PMD tolerance may be achieved at a given performance level as the number of iPCs is increased from 1 to 31. Detailed results verify that the length of the segment to be compensated, rather than the total transmission distance, determines the impact of PMD and as predicted by a simple amendment to the model presented in [17].

2. Effects of PMD on non-linear compensation capabilities of phase conjugation

There are several analytical models for nonlinear transmission performance [17–20], which accurately account for inter-channel nonlinear interactions. If we consider a generalized format for the nonlinear Shannon limit and include the dominant interaction between the signal and amplified spontaneous emission (parametric noise amplification), but neglecting signal depletion [21] effects and other noise dependent terms [22], then the nonlinear signal to noise ratio is given by [13, 15, 17, 23]:

$$SNR_{NL} = \frac{P_s}{NP_N + \eta_{WDM}(1-\eta_P)P_S^3 + 3f_{SN}P_nP_S^2}$$
$$\eta_{WDM} = 2\left(\frac{8}{9}\right)\frac{2\gamma^2 L_{span}}{\pi|\beta_2|}\log N \frac{B_S^2}{2f_W} \tag{1}$$

where P_S represents the signal power spectral density, N the number of spans, P_N the amplified spontaneous emission power spectral density generated by each span, f_{SN} represents the length dependent scaling of parametric noise amplification [15], η_{WDM} is the nonlinear noise scaling

coefficient for lossless transmission, γ is the nonlinear coefficient of the fibre, β_2 the dispersion coefficient, B_s the total WDM signal bandwidth (assuming a continuous spectrum), f_W the nonlinear phase matching bandwidth [13, 17], L_{span} is the length of each fibre span, and η_p represents the efficiency of nonlinear compensation in the presence of PMD where $\eta_p{=}1$ corresponds to ideal nonlinearity compensation where all of the signal-signal interactions have been compensated and $\eta_p = 0$ represents the condition where no nonlinearity compensation is employed. For intermediate values, the amount of signal-signal non-linearity compensated will be given by $\eta_{WDM}(1-\eta_p)$.

Signal-signal nonlinear effects generated in an odd numbered segment (iPC spacing) are compensated in the immediately subsequent even numbered segment. If the compensation is ideal only a final odd numbered segment would contribute to the detected nonlinear noise. However, to first order, any uncompensated nonlinearity within a given pair of segments propagates without further distortion, each pair of segments contributing to the detected nonlinear noise. It is assumed that each such contribution is an independent random variable. However, for the case of signal-noise nonlinear effects, the ideal cancellation of nonlinearity by a pair of segments is only possible for spontaneous emission noise generated at the input to the segment (i.e. from the first amplifier). The residual noise from signal-noise interaction generated within a given pair of segments will of course be considered as an input to all remaining segments and so no further net nonlinear amplification occurs if the compensation is ideal [24]. For simplicity we neglect the impact of imperfect compensation in subsequent spans, since for strong (but incomplete) compensation the additional noise is much smaller than the nonlinear noise generated by a given pair of segments, whilst for weaker (or negligible) compensation nonlinear noise from the residual signal-signal interactions will dominate.

In this way, the nonlinear compensation efficiency is only degraded by the PMD induced, frequency dependent, polarization walk off from one segment rather than from the entire system length. To quantify this degradation, we model the impact of PMD for any link on the efficiency of nonlinearity compensation by following a full statistical analysis [13]. Since we assume that the segments on either side of any given iPC are compensated independently of each other, the influence of birefingence on nonlinearity compensation only accumulates over the inter iPC segment length of $L/(N_{iPC}+1)$,(assuming uniformly spaced iPCs). Following this hypothesis the normalised nonlinear compensation efficiency is

$$\eta_P = \sum_{s=1}^{\frac{N}{N_{iPC}+1}} \frac{3(Ei(-3s\zeta B_s^2) - Ei(-3s\zeta f_w^2)) + (Ei(-7s\zeta B_s^2) - Ei(-7s\zeta f_w^2))}{4NL_{span}\log\frac{B_s^2}{f_w^2}}$$

$$\zeta = \frac{\pi^3 L_{span}\sigma_p^2}{64}$$

(2)

where ζ is the normalised inverse PMD bandwidth, σ_P represents the PMD parameter, N_{iPC} the number of inline phase conjugations and $Ei(.)$ is the exponential integral defined as $Ei(x) = -\int_{-\infty}^{x} e^t/t \; dt$. To represent the shorter compensation length, the summation runs over the number of spans between iPCs. This is equivalent to scaling the PMD coefficient, thus for a given minimum compensation efficiency the acceptable PMD is predicted to be proportional to $\sigma_p/\sqrt{N_{iPC}+1}$. In the following section we use numerical simulations to show that iPC reduces not only parametric noise amplification (as observed previously [23]) but also the detrimental impact of PMD on the nonlinear noise compensation efficiency.

3. Simulation set-up

In order to investigate the effects of PMD, numerical simulations (Fig. 1) were performed using five polarization multiplexed QPSK Nyquist WDM signals (central channel $193.1\,THz$) over a

transmission link comprising thirty two 80 km spans of standard single mode fiber using various numbers of ideal optical phase conjugation devices, distributed uniformly along the link. The transmitter and transmission link were implemented in *VPI TransmissionMaker*9.3 simulated with 2^4 samples per symbol per polarisation (≈ 0.9 THz simulation bandwidth). Ideal lossless Raman amplification and zero dispersion slope are assumed to allow the results to focus on the detrimental impact of PMD without being obscured by power-dispersion symmetry [4]. To increase accuracy of the parametric noise amplification, which is dependent on the point at which amplified spontaneous emission is generated, noise was added every 2.5 *km*. Other fibre parameters are dispersion of $16 ps/(km\ nm)$, a nonlinear coefficient of $1.13\ (W\ km)^{-1}$ and a background loss of $0.046\ km^{-1}$.

The simulation uses standard techniques for calculation polarization effects called "coarse step". In this method the continuous variations of birefringence is substituted by series of many short sections with constant birefringence. The axis of local birefringence varies from section to section. It means that polarization state of the optical field is scattered to a new point on the Poincaré sphere. Artificial periodicities are avoided by choosing a scattering section length from a Gaussian distribution much greater than the correlation length of the fiber birefringence ($50 m$) and shorter than the fibre length. This ensures a large number of scattering events. Each scattering section is defined by frequency dependent Jones matrix which defines the rotation of polarization vector on the Poincaré sphere. The angle of rotation is chosen using a uniform random variable and a biasing factor related to the accumulating PMD value [25,26]. In order to maintain accuracy of the simulation even at very high power, the split step Fourier step was set such that maximum phase change per step was 0.05 *deg* which allowed for variable step sizes related to the amount of nonlinearity being simulated. This allowed from shorter simulation time at lower power levels while maintaining the same accuracy. Each nonlinear step included many polarization scattering sections.
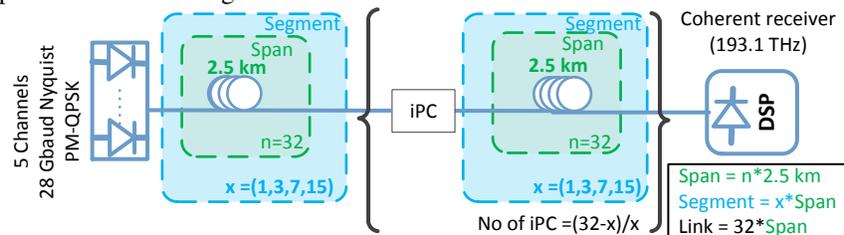

Fig. 1. Simulation set-up consisting of 5 Nyquist shaped 28 Gbaud DP-QPSK channels on 33 GHz grid transmitted over $32x80km$ spans with regularly spaced inline phase conjugation. The iPC spacing was either $1, 2, 4, 8\ or\ 16$ spans resulting in $31, 15, 7, 3, 1$ iPCs.

In the transmitter 28 Gbaud Nyquist shaped signals with a roll off factor of 0.01 were simulated, with 2^{10} bits per polarization and per wavelength (33 GHz spaced wavelengths). An ideal model of the inline optical phase conjugator was used with practical realisation impairments, such as excess losses and crosstalk, neglected also to enable us to focus on the impact of PMD. The iPCs were implemented by reversing the sign of the imaginary field components using a *Matlab* 2015b cosimulation. The iPCs were placed at intervals of 16,8,4,2 and 1 spans. By using an odd number of uniformly spaced iPCs, dispersion was completely compensated and therefore, the dispersion compensation block in the receiver DSP could be bypassed. The WDM spectrum is conjugated about the central channel $193.1\ THz$ and thus there in no effective wavelength conversion of the central wavelength. In the receiver, WDM spectrum was conjugated to ensure that there was no effective wavelength conversion.

Ten simulation runs per point were performed with different random number seeds for each 2.5 km section determining both polarisation rotation and for each spontaneous emission noise.
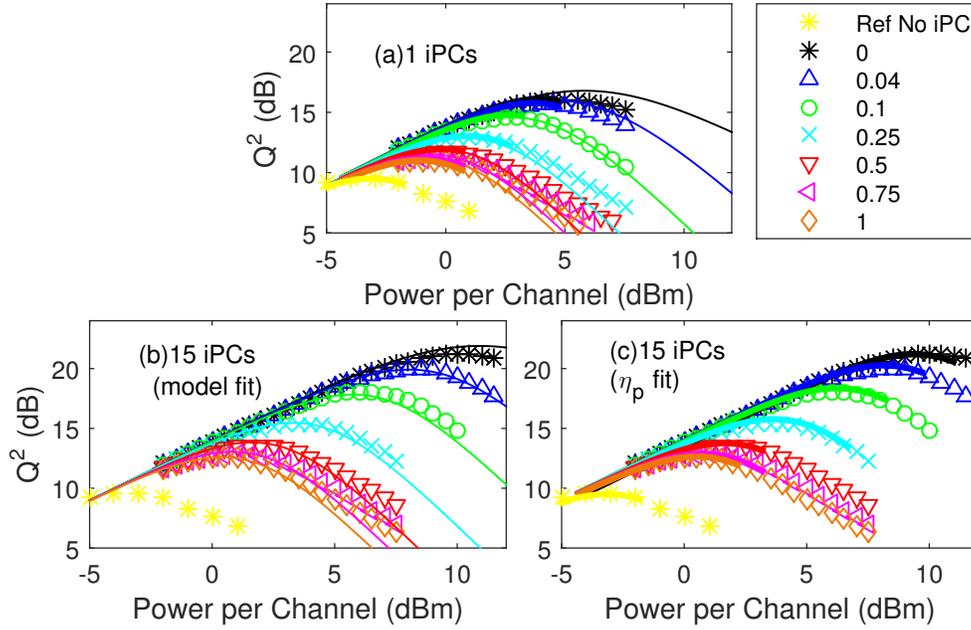
Fig. 2. Plot of performance, Q^2_{dB}, for uniformly spaced ideal iPCs with respect to average PMD (open symbols for $0.04, 0.1, 0.25, 0.5, 0.75, 1 ps/\sqrt{km}$ as detailed in the legend) and increasing launch power (0.5 dB resolution) per channel for $32x80km$ transmission and for reference transmission without iPC (yellow stars). Thin solid lines represent predictions of the analytical model (equations 2 and 3), whilst thick solid lines correspond to arbitrary fitting of results using η_p as the fitting parameter. Graph (a) mid-link iPC performance overlaid with both the analytical model and arbitrary fit (b) performance for 15 iPCs with analytical model and (c) shows 15 iPCs with arbitrary fitting parameter η_p).

The Q^2-factors and delta Q^2-factors presented in this work are calculated from the average of these runs which have a spread of $\pm 0.3 dB$. After coherent detection, the receiver DSP was implemented in Matlab. The received signal was down-sampled to 2 samples per bit and filtered using a matched filter. For reference uncompensated transmission, chromatic dispersion was first compensated using a fixed frequency domain equalizer. The signal was then polarization demultiplexed using a 5 tap butterfly filter, optimized using a constant modulus algorithm. Phase recovery was performed using a Viterbi-Viterbi algorithm with a averaging window of 21. Performance is illustrated by the Q^2-factor of the central channel estimated from the constellation diagram [27].

4. Numerical simulation results

Figure 2(a) shows the performance for a single mid link iPC for various values of PMD. In the absence of PMD a substantial increase in performance (slightly more than 50% of the Q^2_{dB} factor without nonlinearity compensation) and an associated increase in optimum launch power can be observed, as expected for a parametric noise amplification limited system [23]. Figure 2(b) shows results overlaid with analytical model presented in Section 2 and (c) shows the same results overlaid with η_p fit. For each configuration (amount of PMD and number of iPCs), we calculate the fraction of the signal-signal nonlinearity compensated (η_p fit) by fitting the nonlinear threshold curve to Eq. 1 varying only η_p . Since in the region of interest, the performance is dominated by residual inter-signal nonlinear noise, signal-noise interaction can be neglected ($f_{SN} = 0$) which reduces Eq. 1 to ($SNR_{NL} \approx P_s/(NP_N + N\eta_{WDM}(1 - \eta_P)P_S^3)$ where P_N is fit to the linear slope of all curves. A good match between the analytical predictions
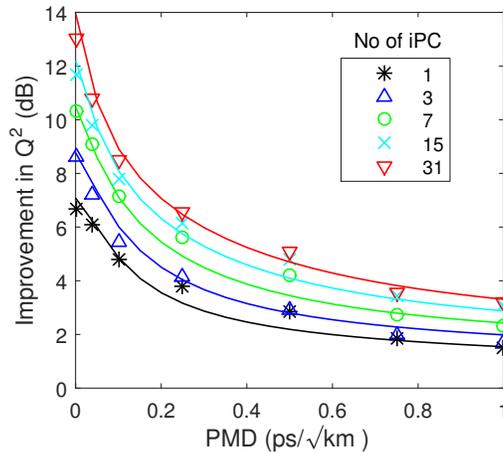
Fig. 3. Graph (dots) shows maximum improvement of Q_{dB}^2 with respect to PMD compared to transmission with digital dispersion compensation only. The solid lines show the fit to full statistical model [13]

and the numerically simulated performance is achieved, except in the high power region for a small number of cases. Slightly better agreement is obtained by fitting η_p, rather than using the analytically predicted value. The benefit of the iPC is eroded by increasing PMD. As the PMD increases, the optimum launch power and maximum achievable performance approach that of the reference transmission with no iPC. This illustrates how PMD effectively breaks the symmetry of the link by randomising the orientation of interacting signals. The optimum launch power reduces from 4.5 dBm to -1 dBm; and the achievable Q_{dB}^2 reduces by 5.2 dB as the PMD increases for 0 to 1 $ps/\sqrt{km}$. As the net performance gain is only 2 dB (comparable to some high performance digital back propagation solutions), this could seriously reduce the attractiveness of using iPC in installed systems with high PMD, although with typical PMD values of around 0.1 $ps/\sqrt{km}$ the performance gain remains attractive for this system.

It has previously been shown that using multiple iPCs results in an increase in the achievable Q_{dB}^2 [23] where multiple iPCs were shown to disrupt the build up of parametric noise amplification. Figure 3 shows the optimum performance improvement for each configuration simulated and confirms that the performance difference decreases with increasing PMD, but that it is always increased by adding additional iPCs. In particular, whilst a 6.2 dB increase in performance with 0 $ps/\sqrt{km}$ for a single iPC is observed as the number of iPC increases this performance increase grows significantly to more than 13 dB. The observed additional increase of 6.8 dB is close to the 6.85 dB anticipated theoretically [23]. However, as the PMD is increased to 1 $ps/\sqrt{km}$, the optimum launch power and peak performance both reduce significantly (from over 7 dB to a little under 2 dB). This is consistent with SNR improvement (lines in Fig. 3) predicted analytically in Section 2 . Importantly however it may be seen that compensation penalties arising from increased PMD may be offset by increasing the number of iPCs included in the transmission link. For a 4 dB performance gain, significantly exceeding the gain available from signal channel DBP [14], the maximum tolerable PMD is a comfortable 0.2 $ps/\sqrt{km}$ using a single iPC. This increases to 0.6 $ps/\sqrt{km}$ for 31 iPCs. Even with a very large PMD of 1 $ps/\sqrt{km}$, 2 and 4 dBm increases in performance are observed when using one and thirty one iPCs respectively. Note that since we have assumed ideal iPCs the impact of ASE noise is unchanged, although the reduction in residual nonlinear noise allows noise limited performance to extend to higher power levels. For extremely high levels of PMD, the performance improvement for all number of iPCs will converge as the symmetry condition will not be met as the rapidly changing polarisation will make the FWM interactions completely
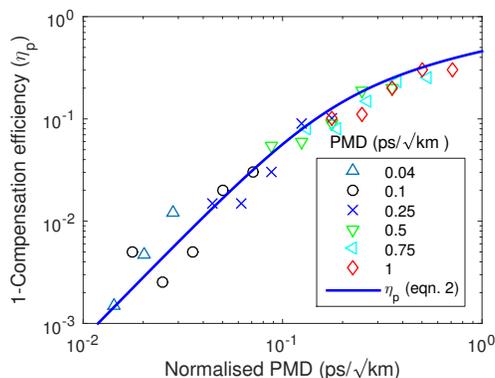
Fig. 4. Nonlinear compensation efficiency as a function of normalised PMD per segment; Solid line - analytically predicted compensation efficiency. Symbols differentiated by PMD coefficient (see legend for details) observed compensation efficiency calculated from curve fits of Eq. 1 to simulated nonlinear threshold curves (eg Fig. 2).

random even over short distances. Overall, we observe that for all levels of PMD studied the performance gain may be doubled by increasing from one to thirty one iPC devices, alternatively, the PMD tolerance may be more than doubled.

For a given transmission fiber (i.e. fixed f_w), the compensation efficiency (η_p) should only depend on the transmission length, PMD and the number of iPCs distributed along the link. To illustrate this our simulation results are directly compared to the analytical predictions in Fig. 4. To enable the comparison for each configuration we calculated np both analytically, or by curve fitting the numerically simulated results to Eq. 1 with η_p as the free parameter. Figure 4 illustrates very good agreement between the analytical estimation and our numerical simulations with no obvious systematic error, effectively confirming that the normalised PMD may be used to directly predict the compensation efficiency.

5. Conclusion

In this work, we confirm that the reduction in nonlinearity compensation efficiency induced by PMD observed for systems using digital back propagation can also disrupt the symmetry required for optimum nonlinearity compensation using inline phase conjugation. However, since each segment of the link (separated by successive iPCs) compensates for the nonlinearity of one of its nearest neighbours by increasing the frequency of iPCs, the transmission distance over which such symmetry breaking may accumulate is proportionally reduced. For the particular system studied, the performance may be improved by up 8.4 dB for a PMD of 0.1 $ps/\sqrt{km}$ by increasing the number of iPCs. Additionally we believe since the nonlinear compensation considered here is modulation format independent, the improvements in PMD tolerance should also be modulation format independent. We further believe that the ability of inline nonlinearity compensators to both disrupt the accumulation of signal-noise nonlinear interactions, and to increase the signal-signal nonlinearity compensation efficiency in the presence of moderate levels of PMD for multiple channels makes them one of the most promising techniques to increase the capacity of future transmission systems.

Acknowledgment